




Research Article

Temperature and power characteristics of quarter-wavelength superconducting coplanar waveguide resonator

Huilong Yu¹ · Lingxiao Jing¹ · Tao Hua^{1,2}  · Weiwei Xu²

Received: 3 November 2021 / Accepted: 17 January 2022

Published online: 02 February 2022

© The Author(s) 2022 [OPEN](#)

Abstract

A quarter wavelength superconducting aluminum film coplanar waveguide resonator with a high-quality factor was designed and fabricated. Furthermore, its resonant frequency and quality as a function of temperatures and exciting powers were investigated. The experimental results showed that the resonance frequency decreases about 1% with the increase of temperature from 50 mK to 1 K, and the load quality factor of the resonator also decreases. The resonant frequency decreases with power from -120 to -70 dBm. The quality factor increases with increased excitation power due to the loss decreases and nonlinearity. The results are consistent with the theoretical analysis of the surface impedance model.

Keywords Superconducting · Coplanar waveguide resonator · Transmission characteristics

1 Introduction

In recent years, superconducting coplanar waveguide (CPW) resonators have been widely used in weak signal detection because of their fast operation, long coherence time, simple structure, and easy integration [1–5]. The high-quality on-chip CPW resonators have been found prominent applications in superconducting electronic circuit devices, such as filters, resonators and sensors et al. With the development of superconducting quantum information technology, a simple layer and balanced structure of the CPW made these CPW resonators widely used to filter or enhance qubit circuits coupling and measure the cosmic background radiation [6, 7]. It is necessary to clarify that physical properties include the frequency and Q factor of the CPW resonator, which are affected by temperature and power.

There are several typical design schemes of the CPW resonator capacitively coupled to the transmission lines, such as half-wavelength resonator, which is coupled by capacitors at each end to input and output ports [8–11], or 1/4-wavelength resonator, which could be coupled to the transmission line by capacitors or inductors using one port and the other end is shorted to ground planes. The cavity quantum electrodynamic experiments include microwave photons and superconducting qubits, have been successfully demonstrated in a superconducting microwave resonator. Great efforts have been made to improve the CPW performance for building multi-qubits processors with large-scale integrated resonator array.

In this paper, a capacitively coupled quarter wavelength superconducting coplanar waveguide resonator hung on the transmission line is designed. The sample was easily prepared using e-beam evaporation and

Huilong Yu and Lingxiao Jing have contributed equally to this work.

✉ Tao Hua, huataonju@163.com | ¹School of Information and Communication Engineering, Nanjing Institute of Technology, Nanjing 211167, China. ²Research Institute of Superconductor Electronics, School of Electronic Science and Engineering, Nanjing University, Nanjing 210093, China.



SN Applied Sciences

(2022) 4:67

| <https://doi.org/10.1007/s42452-022-04956-7>

SN Applied Sciences
A **SPRINGER NATURE** journal

photolithography. The resonant frequency and quality of the device as a function of temperatures and exciting powers were investigated using a vector network analyzer in a dilution refrigerator. We will show that the resonator's resonant frequency and quality factor can be shifted down by increasing the temperature.

2 Sample design and preparation

The geometry of the capacitively coupled CPW resonator is shown in Fig. 1. The length of the resonator determines the frequency of the resonator. The relationship between resonant frequency f_0 and wavelength $4L$ was obtained through [12, 13]:

$$f_0 = \frac{c}{4L} \sqrt{\frac{2}{\epsilon_r + 1}}, \tag{1}$$

where L is the design length of the central conductor, c is light speed, ϵ_r is relative dielectric constant.

The coupling between the resonator and the external transmission line adopts the capacitance coupling of an interdigital structure [14, 15]. And the coupling capacitance between the CPW cavity and the external transmission line affects the loaded quality factor of the resonator and the resonant frequency of the whole resonator. The width of the central conductor is 20 μm , the gap width between the central conductor and the reference ground plane is 10 μm , and the design length of the central conductor is 3.68 mm. The finger length of the insertion

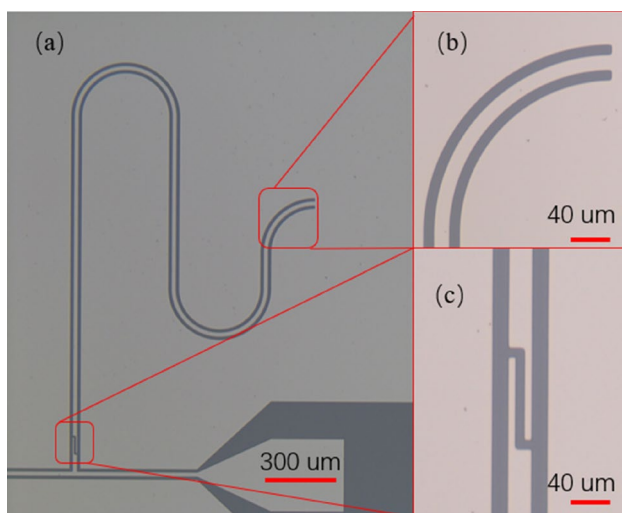


Fig. 1 Optical photos of resonator structure. **a** Resonator sample. **b** Ground terminal of the resonator. **c** Micrograph of a coupling capacitance

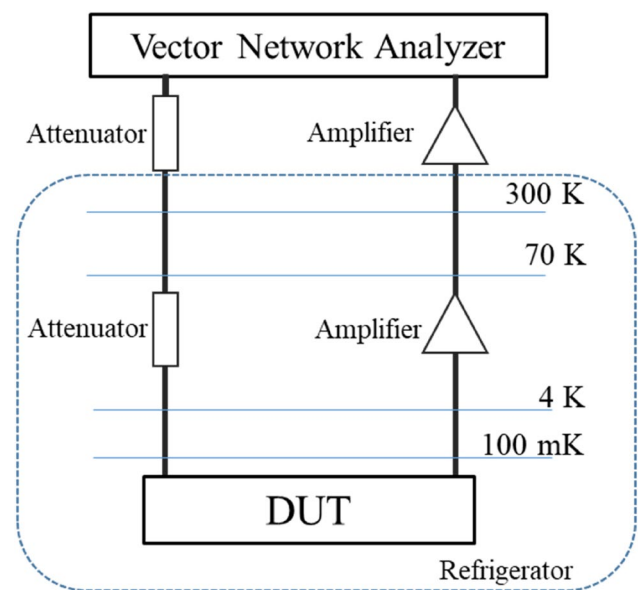


Fig. 2 Schematic diagram of measurement setup

capacitance is 70 μm , the gap is 5 μm , and the coupling capacitance is about 1.55 fF.

The resonator sample was prepared on a pure high-resistivity (>8000 Ωcm) 2-inch silicon wafer with a substrate thickness of 500 μm . The fabrication processes are as follows. First, an Al film ($T_c \approx 1.2 \text{ K}$) of about 70 nm was evaporated on the cleaned silicon substrate by electron beam evaporation. Then, The CPW resonator was patterned with optical lithography. After developing 30 s in ZJX-238 developer and post-baking, the Al was etched away using wet etching in a mixture solution of deionization water and ZJX-238 developer solution (6:1) for about 7 min at room temperature. Figure 1a shows a coplanar waveguide resonator after stripping resistance. Then the chips are diced into 4 mm×4mm squares. Figure 1b is the short-terminal of the resonator. And Fig. 1c is the coupling capacitance of the resonator, which is equivalent to establishing a channel between the circuit and the resonator, so that the S_{21} coefficient of the resonator can be measured.

3 Measurement results and analysis

We placed the sample in a dilution refrigerator and cooled it to 50mK to keep the sample in a superconducting state. S_{21} transmission measurements of the resonator were performed in a dilution refrigerator system at a base temperature varying from 1 K to 50 mk. The microwave setup is shown in Fig. 2. The input line includes room temperature and cold attenuators used to reduce thermal noise on a signal line. Furthermore, the output line includes an

amplifier (55 dB) connected to balance the measurement circuit and amplify the signal at room temperature.

First, we measured the S_{21} of the transmitted signal using a network analyzer (Agilent N5222A) with IFBW=10 kHz to extract the resonator frequency and quality factors dependence of temperature. As shown in Fig. 3, the resonant frequency (inset) was depicted as a function of the base temperature. The experimental results showed that the resonance frequency decreases about 1% with the temperature increase from 50 mK to 1 K. The temperature change leads to the change of surface impedance which causes the resonant frequency shift. The resonant frequency f_0 is given by [16].

$$\frac{\Delta f_0}{f_0} = -\frac{\alpha \Delta X_s(T)}{2X_s} = \frac{\alpha \Delta \sigma_2(T)}{2\sigma_n}, \quad (2)$$

where f_0 is the resonant frequency, kinetic inductance factor α is the ratio of the kinetic inductance to the total inductance of the resonator. X_s is the surface reactance of the resonator, σ_2 is the imaginary part of film electroconductivity, σ_n indicates the normal state of conductivity. In Eq. (2), the increase of temperature makes σ_2 smaller. The surface impedance increases, which shifts the resonant frequency decreased.

The measured resonator frequencies are fitted to the theoretical calculation values shown in Fig. 3. Kinetic inductance factor α is 0.036 in Eq. (3). The resonant frequency agrees with the surface impedance model. We also compared the relative offsets of resonant frequency under different power excitation. The result indicates that the frequency shift of the resonator is mainly determined by the change of the surface impedance with temperature.

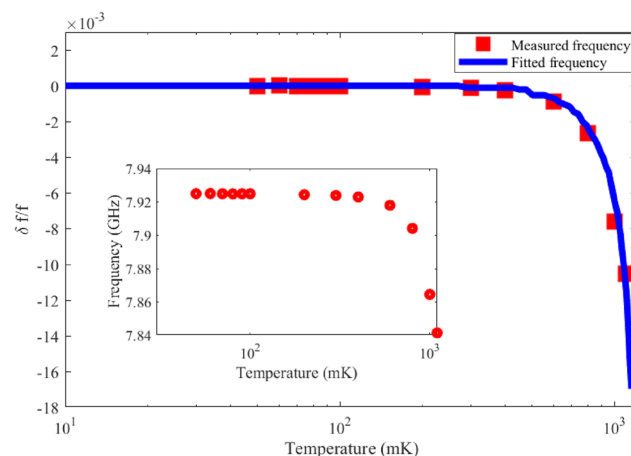


Fig. 3 The relative shift of resonant frequency versus temperature, and the measured resonant frequency as a function of the temperature (inset)

In addition, we measured the dependence of the temperature on the load quality factor of the resonator. As shown in Fig. 4, the inset figure shows the load quality factor Q measured in the dilution refrigerator base temperature from 50 mK to 1 K at excitation power of -120 dBm. As the temperature increases, the load Q value decreases, which can be explained by the change of surface impedance with temperature; the load quality factor Q_r is given by [16]

$$\Delta \frac{1}{Q_r} = \alpha \frac{\Delta R_s(T)}{X_s} = -\alpha \frac{\Delta \sigma_1(T)}{\sigma_n}. \quad (3)$$

where Q_r is the load quality factor, R_s is the surface resistance of the resonator, σ_1 is the real part of film electroconductivity, and σ_n indicates the normal state of conductivity. Using the α obtained from Eq. (2), we calculated the relative shift of load Q_r value with temperature change. The results show that the load quality factor of the resonator decreases with the increase of temperature.

We can also measure the effect of loss and nonlinearity contributing to the system by comparing the quality factors between low and high power at any specified temperature. The resonant frequency and load quality factor dependence of excitation power at different temperatures are depicted in Fig. 5. The measured Q of the device varied enormously with the increase of excitation power from -120 to -70 dBm stepped by 5 dBm at the base temperature of 60 mK. Moreover, the resonator frequency does not increase correspondently but decreases and tends to be stable. The measured result indicated high power to minimize dielectric loss but low enough to avoid nonlinearities, which shifted the frequency down, and as input power increased, the loss decreased, and the impact of

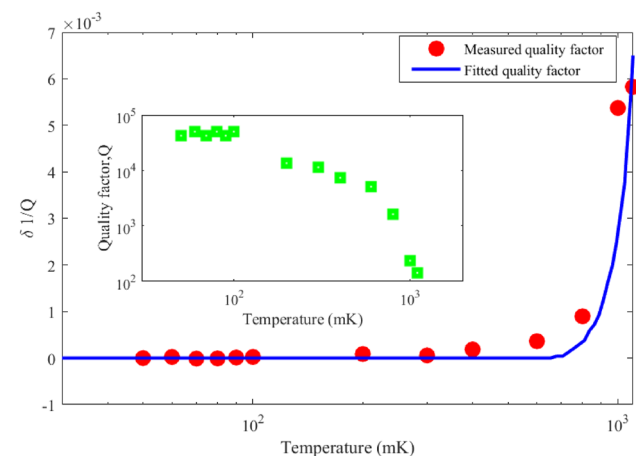


Fig. 4 The relative shift of measured and fitted quality factor with different temperature, and the measured quality factor as a function of the temperature (inset)

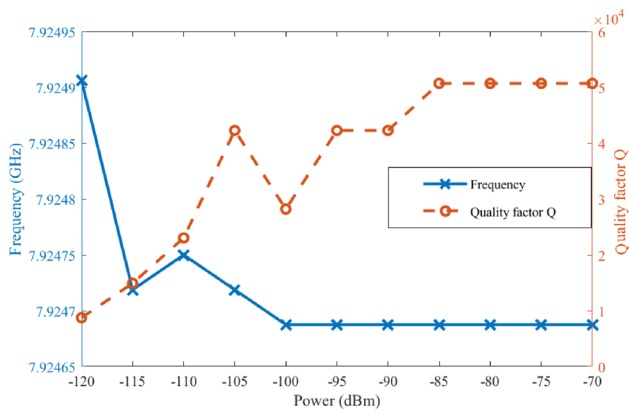


Fig. 5 Resonant frequency and load quality factor with different excitation power under the temperature of 60 mK

loss on the system was reduced. The Q factor will increase accordingly.

4 Conclusions

We have designed and fabricated a quarter wavelength superconducting coplanar waveguide resonator and measured its low temperature superconducting transmission characteristics using a vector network analyzer.

The experimental results showed that the resonator frequency would shift to the low-frequency direction with increasing temperature under surface impedance and kinetic inductance. The excitation power also significantly influences the quality factor and resonant frequency. However, the relative variation of load quality factor and resonant frequency agree with the surface impedance model. The experimental results are helpful for the design and implementation of CPWs.

Funding The funding was provided by the National Natural Science Foundation of China (Grant Nos. 61501222, 61727805, and 61701219), and the School Scientific Research Fund of Nanjing Institute of Technology (Grant No. CKJA201904, CKJB201803).

Declarations

Conflict of interest On behalf of all authors, the corresponding author states that there is no conflict of interest. I am the author responsible for the submission and the Springer OA License Agreement as detailed above.

Open Access This article is licensed under a Creative Commons Attribution 4.0 International License, which permits use, sharing, adaptation, distribution and reproduction in any medium or format, as long as you give appropriate credit to the original author(s) and the source, provide a link to the Creative Commons licence, and indicate if changes were made. The images or other third party material in this article are included in the article's Creative Commons licence, unless indicated otherwise in a credit line to the material. If material is not

included in the article's Creative Commons licence and your intended use is not permitted by statutory regulation or exceeds the permitted use, you will need to obtain permission directly from the copyright holder. To view a copy of this licence, visit <http://creativecommons.org/licenses/by/4.0/>.

References

- Murray CE (2020) Analytical modeling of participation reduction in superconducting coplanar resonator and qubit designs through substrate trenching. *IEEE Trans Microw Theory Tech* 99:1–1
- Goeppl M, Fragner A, Baur M et al (2008) Coplanar waveguide resonators for circuit quantum electrodynamics. *J Appl Phys* 104(11):283
- Lahtinen V, Möttönen M (2020) Effects of device geometry and material properties on dielectric losses in superconducting coplanar-waveguide resonators. *J Phys Condens Matter* 32(40):405702
- Ding JQ, Hu J (2021) Shi.350-GHz bandpass filters using superconducting coplanar waveguide. *IEEE Trans Terahertz Sci Technol* 11(9):548–556
- Nagai M, Murayama Y, Nitta T et al (2020) Resonance spectra of coplanar waveguide MKIDs obtained using frequency sweeping scheme. *J Low Temp Phys* 199(1):250–257
- Baselmans J, Barends R, Hovenier JN et al (2005) High Q Niobium superconducting resonators for use as Kinetic Inductance sensing elements. In: *Proceedings of the European interferometry initiative workshop organized in the context of the 20005 Joint European and National Astronomy Meeting "Distant Worlds"*
- Wang Y, Zhou P, Wei L et al (2013) Photon-induced thermal effects in superconducting coplanar waveguide resonators. *J Appl Phys* 114(15):38–46
- Hayashi K, Saito A, Sawada T et al (2013) Microwave characteristics of microwave kinetic inductance detectors using rewrap spiral resonators array. *Phys Procedia* 45:213–216
- Zhou K, Ren L, Shi J et al (2020) Feasibility study of optical fiber sensor applied on HTS conductors. *Phys C Supercond* 575:1353693
- Shen B, Geng J, Zhang X et al (2017) AC losses in horizontally parallel HTS tapes for possible wireless power transfer applications. *Physica C (Amst, Neth)* 543:35–40
- Morgan AA, Hogan SD (2020) Coupling rydberg atoms to microwave fields in a superconducting coplanar waveguide resonator. *Phys Rev Lett* 124(19):193604
- Calvo M (2008) Development of kinetic inductance detectors for the study of the cosmic microwave background polarization. Ph.D. thesis, Sapienza university in Roman
- Mazin BA (2004) Microwave kinetic inductance detectors. Ph.D. thesis California: California Institute of Technology Pasadena
- Clem JR (2013) Inductances and attenuation constant for a thin-film superconducting coplanar waveguide resonator. *J Appl Phys* 113(1):169-R
- Hofheinz M, Wang H, Ansmann M et al (2009) Synthesizing arbitrary quantum states in a superconducting resonator. *Nature* 459(7246):546–549
- Gao J (2008) The physics of superconducting microwave resonators. Ph.D. thesis California California Institute of Technology Pasadena

Publisher's Note Springer Nature remains neutral with regard to jurisdictional claims in published maps and institutional affiliations.